Journal of Fluorescence, Vol. 11, No. 4, December 2001 (© 2002)

Fluorescence Lifetime Distribution in Characterizing Membrane Microheterogeneity

G. Krishnamoorthy[1,2] and Ira[1]

Realistic description of biomembrane heterogeneity is essential for understanding the complexity of their function. Application of the distribution of the fluorescence lifetime of membrane probes, especially by the maximum entropy method, in studying membrane heterogeneity is described. Representative studies on various membranes and the information brought out in these studies are reviewed. An example is provided wherein the water-wire hypothesis of transmembrane proton transport gets experimental support from Nile Red fluorescence lifetime distribution analysis. Future directions in the use of this methodology in cell physiology are indicated.

KEY WORDS: Fluorescence lifetime distribution; maximum entropy method; membrane microheterogeneity; time-resolved fluorescence microscopy.

INTRODUCTION

The dictum that structure and dynamics control the function of macromolecular systems is quite appropriate in the case of biological membranes. The static picture of membranes visualized as barriers enclosing various cellular compartments [1] is being replaced by a dynamic and heterogeneous description. The heterogeneity could be present in both spatial and temporal domains. Spatial heterogeneity is exemplified by microdomains of sizes ranging from nanometers to several hundred micrometers [2–4]. Nanometer-sized microdomains have been postulated as control elements in a variety of cellular processes such as signal transduction, membrane trafficking, receptor internalization, and cell fusion [5,6]. Heterogeneity in the temporal domain could control processes such as transmembrane transport and cell division.

The heterogeneity of membranes' structure, while forming the basis of their function, precludes the application of X-ray crystallography and high-resolution NMR for determining their structure. (However, magic angle spinning NMR studies have given structural information on oriented membranes [7–9].) Hence, a large variety of spectroscopic techniques has been applied for determining the structure and dynamics of membranes. Fluorescence is the most widely used spectroscopic technique due to its high sensitivity and selectivity. The application of fluorescence-based techniques has been covered in several recent reviews [10]. In this article we review the applications of fluorescence lifetime distribution in characterizing the dynamics and heterogeneity of membranes. Despite its strong potential, this technique has not been applied as extensively as many other techniques.

FLUORESCENCE LIFETIME DISTRIBUTION

The lifetime distribution of fluorescence probes is a powerful method for characterizing complex systems such as membranes. Fluorescence decay kinetics of probes distributed in complex systems generally show a considerable level of heterogeneity. It is reasonable to assume that, in the absence of evidence on the number

[1] Department of Chemical Sciences, Tata Institute of Fundamental Research, Homi Bhabha Road, Mumbai 400 005, India.
[2] To whom correspondence should be addressed. E-mail: gk@tifr.res.in Fax: +91-22-215 2110.

1053-0509/01/1200-0247/0 © 2002 Plenum Publishing Corporation

of populations (however, see Refs. 11 and 12), the probe is distributed into a very large number of populations whose properties could vary from each other. In such situations, fitting the observed decay kinetics to a distribution of lifetimes is more rational than fitting them to a sum of a few (three or fewer) discrete exponentials.

Fluorescence intensity [$I(t)$] decay kinetics can be represented by the general expression

$$I(t) = \int_0^\infty \alpha(\tau)\exp(-t/\tau)d\tau \quad (1)$$

where τ is the fluorescence lifetime and the function $\alpha(\tau)$ represents the distribution of lifetimes. In the case of discrete lifetimes, the right-hand side becomes $\Sigma\alpha_i \exp(-t/\tau_i)$ where α_i is the amplitude of the ith lifetime component (τ_i).

There are several ways in which distributions of lifetimes can be described in real systems. The use of Gaussian or Lorentzian functional forms for describing the shape of lifetime distributions [$\alpha(\tau)$] has been popular in proteins [13–15] and membranes [16,17]. Despite their wide applications, these functional forms do not have any clear physical basis (see below). Further, the fixation of modality (unimodal, bimodal, etc.) of distribution functions has also been largely arbitrary [15]. In contrast, analysis of fluorescence decay kinetics by the maximum entropy method (MEM) [18–20] is virtually model-free and hence is expected to offer the most realistic description of complex systems.

MAXIMUM ENTROPY METHOD

MEM starts with a flat distribution of $\alpha(\tau)$ with no bias on any functional form. The only assumption invoked is that $\alpha(\tau)$ is represented initially by the sum of a few hundred exponentials. Analysis consists of modifying α_i in each iteration such that minimization of χ^2 and maximization of Shannon–Jaynes entropy (S) occur [20].

$$\chi^2 = \frac{\sum_{i=1}^{n} W_i[I(t_i) - I_c(t_i)]^2}{n_2 - n_1 + 1 - p} \quad (2)$$

where, for n data points, W is a weighted factor for the ith data point, n_1 and n_2 are the first and last channels of the decay, and p is the number of variable parameters. $I(t_i)$ is the fluorescence intensity for the ith data point and $I_c(t_i)$ is the calculated fluorescence intensity for the same.

$$S = -\sum \alpha_i \log \alpha_i \quad (3)$$

For a particular value of χ^2 there can be many possible patterns of $\alpha(\tau)$. MEM identifies the distribution pattern for which S is maximum. MEM gives a continuous distribution of lifetimes as the required solution without assuming any model or mathematical function. The solution given by MEM is a general one, which also includes the solution obtained by a discrete sum of a few exponentials. If the decay is truly the sum of N exponentials (representing N populations), then MEM will generate a distribution with N peaks provided that the signal-to-noise ratio is sufficient to resolve the peaks [20].

The following features of lifetime distributions could be used to gain information on the system: (i) the number of peaks, (ii) the position of the peaks, (iii) the width of each distribution, and (iv) the shape of the distribution. The width has been shown to depend upon factors such as the signal-to-noise ratio, completeness of data collection, discretization in τ space, and χ^2 stopping criterion, apart from the width originating from the heterogeneity of the sample [20]. Hence to interpret the width of distributions it is essential to examine the effect of such analysis-related artifacts.

Analysis of fluorescence decay kinetics by MEM is useful even in situations where the interpretations are based on the results obtained from analysis by the sum of a discrete number (three or fewer) of exponentials. When MEM analysis results in a number of peaks, the peak positions and their relative integrated intensities matching the values of τ_i and α_i obtained from discrete analysis, one can have confidence in interpreting the observations based on the discrete values of τ_i and α_i. Thus, MEM could be used to validate discrete exponential analysis. This would be useful in situations where rapid analysis of fluorescence decay kinetics is required. However, information on the heterogeneity of the system is largely hidden in discrete lifetime analysis.

LIFETIME DISTRIBUTION IN MEMBRANES

The width and peak position of fluorescence lifetime distributions of a variety of fluorescence probes have been used in characterizing both lipid [16,21,22] and natural [23,24] membranes. DPH and DPH derivatives have been the probes of choice in most of these studies. Also, either unimodal or multimodal Lorentzian or Gaussian functional forms have been used in analyzing fluorescence decay kinetics in most experiments [16,21,23,24], although MEM has been used is a few cases [22,25–27].

By employing Lorentzian distribution analysis several workers came to the conclusion that polyunsaturated lipid membranes become more homogeneous in the presence of cholesterol [16,21]. In these cases the widths of lifetime distributions of DPH and its derivatives decreased with the increase in the level of cholesterol. In contrast, when Nile Red was used as the probe and the decay kinetics of fluorescence was analyzed by MEM, the width of the distribution increased with the increase in the level of cholesterol [25–28]. This behavior was observed in saturated and mixed natural lipid vesicles [26,27] and also in planar supported membranes [27]. These contrasting results could be due to (i) the use of different membrane probes that report different regions of the bilayer and (ii) the use of Lorentzian functional forms versus the use of unbiased MEM in analyzing the fluorescence decay kinetics. As mentioned earlier, MEM analyses are likely to be superior compared to the use of functional forms such as Lorentzian and Gaussian, as there is no physical basis for the latter. It is likely that a combination of both the factors mentioned above is responsible for the contrasting observations. Obviously, more experiments are needed to resolve this issue. Brochon and co-workers [22,29] have used *trans*-parinaric acid and MEM analysis to probe lipid clustering, the coexistence of membrane phases, and the effect of cholesterol. In these cases, MEM analysis has clearly brought out quantitatively the existence of two types of liquid crystalline phases. In view of these studies it is likely that the cholesterol-induced broadening of lifetime distribution seen in MEM analysis of Nile Red fluorescence [25–28] could also be due to the presence of multiple phases. In fact, the presence of a heterogeneous environment around Nile Red in cholesterol-containing membranes was seen from the increase in the width of the emission spectra also (Ira, A. S. R. Koti, G. Krishnamoorthy, and N. Periasamy, unpublished observation). Further, the level of raft formation has been shown to increase in the presence of cholesterol in cell membranes [30], suggesting increased heterogeneity in the presence of cholesterol. In single lipid systems it has been shown by the DPH lifetime distribution [22] that the heterogeneity decreases at higher (e.g., 50%) levels of cholesterol. However, it is unlikely that such a behavior would be seen with mixed lipids. Also, it should be interesting to monitor this using other lipid probes.

Membrane perturbations induced by a variety of agents such as ionizing radiation [31], chronic ethanol intoxication [24], benzyl alcohol [32], and hydrostatic pressure [33] have been analyzed by the Lorentzian distribution of the lifetime of DPH analogues. Apart from the use of extrinsic membrane probes, lifetime distributions of intrinsic fluorophores such as chlorophyll-a in thylakoid membranes have been described [34].

ORIGIN OF THE FLUORESCENCE LIFETIME DISTRIBUTION

The representative examples given above indicate that the distribution of fluorescence lifetimes in membranes is modulated by a variety of factors. Although the width of the lifetime distribution can be taken as an indicator of the level of environmental heterogeneity seen by the probe [28,33] a more quantitative interpretation of the distribution would be useful. Such an interpretation is possible only when factors controlling the experimental lifetime can be identified. Fluorescence lifetime is a highly sensitive parameter and is controlled by a variety of factors. Hence, identification of factors which cause changes in it is not straightforward. However, one could design systems wherein the observed changes could be correlated with the structure and dynamics. One such example is the situation encountered in fluorescence resonance energy transfer (FRET), where the lifetime distribution arises due to the distribution of distance between the donor and the acceptor [15,35]. Intramolecular distance distributions in proteins [35] and in membranes [36] have been derived from lifetime distributions based on either functional forms or the unbiased MEM.

Yeager and Feigenson [37] have performed Monte Carlo simulations of acyl chain occupancy in lipid membranes and generated probability distributions of fluorescence quenchers around the probe. The results of these simulations yielded discrete distributions of fluorescence lifetimes, which were then compared with Gaussian and Lorentzian continuous distributions. It was found that the Gaussian function fits the simulated distributions better than the Lorentzian. Thus, this work supports the use of Gaussian function for fitting the distribution of lifetimes. In this context it should be mentioned that MEM-obtained distributions generally fit fairly well to Gaussian functions. (However, the number of Gaussians used will still remain arbitrary.) Also, it has been pointed out that symmetrical distributions, if used, should apply to the distribution of nonradiative rate constants rather than to fluorescence lifetimes [37,38]. Thus these arguments also bring about, once again, the superiority of MEM, which is model-free. Zimet and co-workers [39] have also used FRET between a donor attached to a membrane protein and an acceptor in the phospholipid and performed Monte Carlo simulations for deriving lifetime distributions under

conditions of crowding in membranes. Their results indicate that the distribution of τ can differ markedly even for systems having the same value of average τ.

CORRELATION OF THE WIDTH OF THE LIFETIME DISTRIBUTION WITH THE MEMBRANE PHYSICAL STATE

Although the width of the lifetime distribution has been used to interpret the integrity and heterogeneity of membranes, there is a paucity of information that relates the observed width (and its changes) to other physical properties of the membrane. It was shown earlier that the width of the lifetime distribution of Nile Red in membranes can track the gel-to-liquid crystal phase (L_α) transition in lipid membranes [25]. The width was significantly greater in the gel phase compared to the L_α phase. Figure 1 shows that this behavior is seen in a number of probes apart from Nile Red, such as Merocyanine 540 and STQ-3. Lipid vesicles made from either DPPC or DMPC at 35°C were used as markers of the gel and L_α phases, respectively. Gel–L_α phase transition temperatures of 42 and 24°C for DPPC and DMPC, respectively, ensure that DPPC and DMPC vesicle membranes are in the gel and L_α phases, respectively, at 35°C. It is interesting to note that BODIPY did not show any significant difference in width. This could be due to its environmental insensitivity (unpublished observations).

Various mechanisms that could explain the observed increase in width of the lifetime distribution in the gel phase were discussed earlier [25,26]. Basically, the larger width in the gel state could be the result of a slower sampling rate for various environments and orientations such that $\tau_F < \tau_S$, where τ_F is the fluorescence lifetime and τ_S is the sampling time, which is related to the mean residence time of the probe. In the fluid L_α state one could have the reverse situation, $\tau_F > \tau_S$. Thus, the larger width in the gel state could represent the collection of individual probe environments. The narrower width in the fluid state could be the result of dynamic averaging of environments. The translational diffusion coefficient (D) of small neutral molecules such as Nile Red in fluid membranes is $\sim 10^{-6}$ cm^2/s [40]. Hence the average distance [$\langle x \rangle = (2D\tau_F)^{1/2}$] traveled during the lifetime τ_F is ~8-Å. In the gel state, D is expected to be smaller, and hence the value of $\langle x \rangle$. This difference in $\langle x \rangle$ could be a major factor in deciding the level of dynamic averaging of environments leading to a larger width in the gel state. Further, probes could be localized in the gel grain boundaries and this could contribute to the increased heterogeneity in the gel phase. On the whole we can conclude that the lifetime distribution in membranes reflects the presence of locations and microenvironments having different polarities and polarizabilities.

The planar supported membrane is a very useful membrane system, both as a model membrane and as an effective matrix for futuristic devices [41]. Characterization of such membranes by the Nile Red fluorescence lifetime distribution revealed significant differences in their physical state compared to vesicle membranes [27]. For example, the gel–L_α phase transition of DMPC, seen by the width of the lifetime distribution in vesicle membranes, is absent in supported bilayers (Fig. 2). It is likely that the physical state of the lipids in the planar bilayer is close to that in the gel state in the observed temperature range (10–35°C).

Bernsdorff and co-workers [33] have obtained distributions of the lifetime of DPH derivatives in DPPC and POPC membranes as a function of the hydrostatic pressure in the range 1–1500 bar. The width of the distribution showed an increase with increases in pressure probably, indicating structural transition.

LIFETIME DISTRIBUTION IN SINGLE LIVING CELLS

Information on the fluorescence lifetime distribution obtained in bulk samples of lipid and cell membrane preparations could be used in modeling similar observations in single living cells under a fluorescence microscope. Such measurements are useful in mapping the membrane properties within a single cell with spatial resolution limited by the optical method. However, unlike maps created from fluorescence intensity, mapping by lifetime distribution requires vastly enhanced data handling and hence it is preferable to perform lifetime distribution analysis on preselected locations in the cell. For example, the Nile Red lifetime distribution in the plasma membrane was found to be significantly broader compared to the nuclear membrane in the same cell [25,26]. This observation is in line with the fact that the cholesterol level is significantly higher in the plasma membrane compared to nuclear membranes [42] and the observation (in vesicle membrane samples) that cholesterol increases the width of the lifetime distribution. Similarly, the widths of distributions were smaller in plant cells compared to animal cells, which is again in line with the fact that the cholesterol level in plant cells is significantly lower. Such correlations could be supported by direct observation of the changes in the width of the distribution when the cells are depleted of their cholesterol content by treatment with methyl-β-cyclodextrin (Fig. 3). Thus this offers a

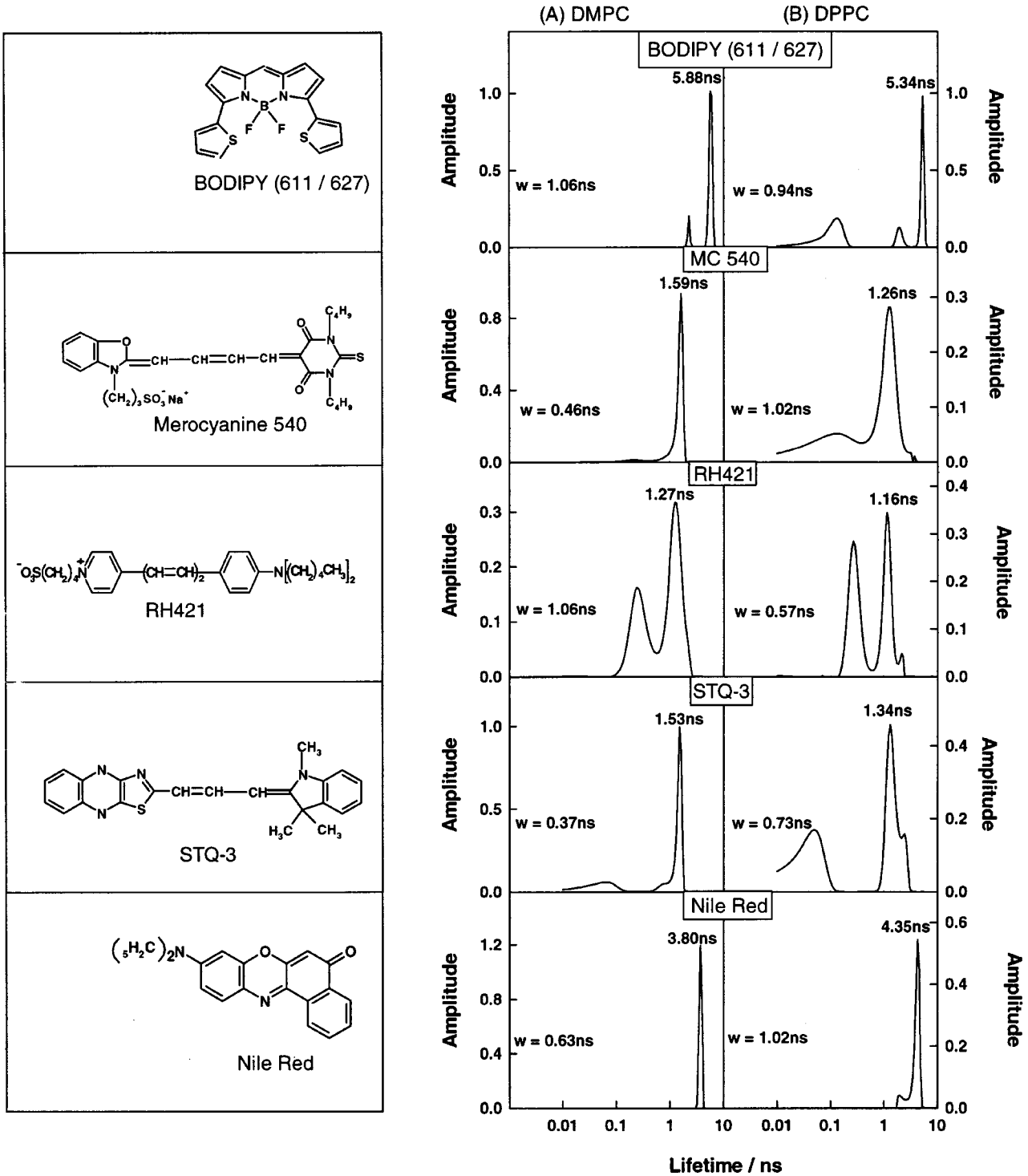

Fig. 1. MEM distribution of various fluorescence probes in DMPC (A) and DPPC (B) vesicle membranes at 35°C. At this temperature, DMPC and DPPC membranes are in the liquid crystalline (L_α) and gel phases, respectively. w—width of the lifetime distribution. The peak positions are marked on the respective distributions.

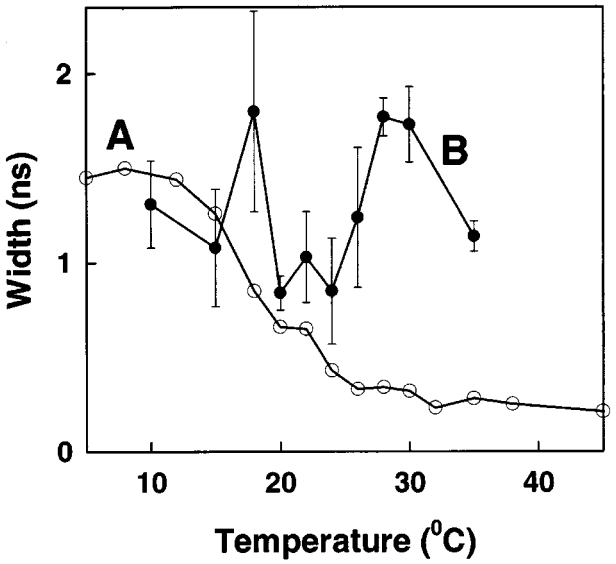

Fig. 2. Temperature dependence of the width of the Nile Red lifetime distribution in (A) DMPC vesicles and (B) DMPC planar supported membranes.

powerful tool for tracking the spatial dependence of membrane properties within a single living cell.

CORRELATION OF LIFETIME DISTRIBUTION WITH MEMBRANE FUNCTION

There is no need to stress the point that the main aim of probing the membrane structure and dynamics is to understand their function. Can we find answers for at least some of the complex behavior of membranes from the lifetime distribution of fluorescence probes? Microdomains in membranes are being recognized as strong candidates for explaining cell functions such as receptor-mediated endocytosis and membrane trafficking [5,6]. Submicron sizes of these domains preclude direct observations by optical microscopy, and hence various spectroscopic techniques such as FRET-induced changes in fluorescence intensity decay [36] and FRET-induced changes in fluorescence anisotropy [30] have been used in characterizing them. The fluorescence lifetime distribution could be used in identifying (i) the extent of microdomains present and (ii) the dynamics of microdomains. Since a combination of these factors dictates the observed lifetime distribution, these could be derived by devising appropriate model systems.

One of the important functions of biological membranes is the selective and controlled transport of ions and molecules across them. Although most transport occurs through specific carriers and channels, information on transport through the lipid part of the membrane is also essential. For example, the permeability coefficient for protons ($P_{H^+} = 10^{-3}$ to 10^{-5} cm/s) is 3–5 orders of magnitude higher than that of Na^+ or K^+ ($P_{Na^+,K^+} = 10^{-8}$ cm/s). Hydrogen-bonded water wires across membranes have been hypothesized for explaining this anomalously high value of P_{H^+} [43,44]. The transient nature of such water wires would add to the heterogeneity and dynamics of the membranes. This could be picked up by the lifetime distribution of fluorescence probes. In a recent study [28]

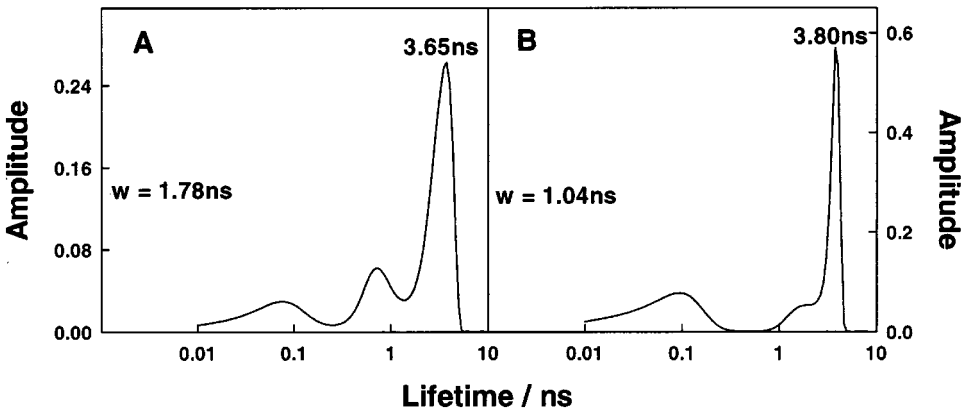

Fig. 3. Effect of cholesterol depletion on the MEM distribution of Nile Red in CHO (TRVb-1) cells. Cells were depleted of cholesterol by incubation with 10 m*M* methyl-β-cyclodextrin in medium 1 (150 m*M* NaCl, 5 m*M* KCl, 1 m*M* $CaCl_2$, 1 m*M* $MgCl_2$, and 20 m*M* HEPES buffer, pH 7.4) at 37°C for ~1 h. The cyclodextrin solution was then washed off with PBS (137 m*M* NaCl, 2.7 m*M* KCl, 8.1 m*M* Na_2HPO_4, 1.5 m*M* KH_2PO_4, pH 7.2) and the cells were loaded with Nile Red in the same medium. (A) Control cells (cells not treated with methyl-β-cyclodextrin); (B) cholesterol-depleted cells. The peak position of the distribution is indicated in the respective plots, and w is the width of the distribution.

we showed that we could obtain a correlation between the proton permeability of membranes and the MEM-analyzed fluorescence dynamics of Nile Red. Proton permeability was modulated by the level of cholesterol. An increase in the level of cholesterol caused the following: (i) a decrease in the level of proton permeability, (ii) an increase in the peak position of the Nile Red lifetime distribution, and (iii) an increase in the width of the distribution [28]. The increase in the peak position reflects, most likely, a decrease in the level of hydration of the bilayer similar to the interpretation with DPH derivatives [45]. Thus, the observed decrease in proton flux is probably caused by a decrease in the level of hydration. This could be taken as strong support for the water-wire hypothesis of proton transport.

CONCLUDING REMARKS

The heterogeneity of complex systems such as biological membranes is best described by an unbiased distribution of its properties. MEM analysis of the fluorescence decay kinetics of membrane probes has been shown to be one such method, which is expected to add to other techniques for describing the contribution of membrane structure and dynamics in eliciting its functions.

ACKNOWLEDGMENTS

We thank Prof. N. Periasamy for providing us with the home-developed software for MEM analysis and for advice on using it effectively. Partial financial support from the Department of Science and Technology, Government of India, toward the time-resolved fluorescence microscopy system is acknowledged. The suggestions of the reviewer are gratefully acknowledged.

REFERENCES

1. S. J. Singer and G. L. Nicholson (1972) *Science* **175**, 720–731.
2. K. Jacobson and C. Dietrich (1999) *Trends Cell Biol.* **9**, 87–91.
3. M. Edidin (1997) *Curr. Opin. Struct. Biol.* **7**, 528–532.
4. O. G. Mouritsen and K. Jorgensen (1997) *Curr. Opin. Struct. Biol.* **7**, 518–527.
5. K. Simons and E. Ikonen (1997) *Nature* **387**, 569–572.
6. N. M. Hooper (1998) *Curr. Biol.* **8**, R114–R116.
7. M. Auger (1997) *Biophys. Chem.* **68**, 233–241.
8. C. Glaubitz and A. Watts (1998) *J. Magnet. Reson.* **130**, 305–316.
9. J. L. Griffin, H. J. Williams, E. Sang, and J. K. Nicholson (2001) *Magnet. Reson. Med.* **46**, 249–255.
10. L. Davenport (1997) *Methods Enzymol.* **278**, 487–512.
11. M. M. G. Krishna and N. Periasamy (1998) *J. Fluoresc.* **8**, 81–91.
12. A. S. R. Koti, M. M. G. Krishna, and N. Periasamy (2001) *J. Phys. Chem. A* **105**, 1767–1771.
13. J. R. Alcala, E. Gratton, and F. G. Prendergast (1987) *Biophys. J.* **51**, 597–604.
14. A. M. Gilmore, V. P. Shinkarev, T. L. Hazlett, and G. Govindjee (1987) *Biophys. J.* **51**, 925–936.
15. A. Navon, V. Ittah, P. Landsman, H. A. Scheraga, and E. Haas (2001) *Biochemistry* **40**, 105–118.
16. Q. T. Li and N. P. Das (1994) *Arch. Biochem. Biophys.* **315**, 473–478.
17. C. P. Sotomayor, L. F. Aguilar, F. J. Cuevas, M. K. Helms, and D. M. Jameson (2000) *Biochemistry* **39**, 10928–10935.
18. J. C. Brochon (1994) *Methods Enzymol.* **240**, 262–311.
19. R. Swaminathan, G. Krishnamoorthy, and N. Periasamy (1994) *Biophys. J.* **67**, 2013–2023.
20. R. Swaminathan and N. Periasamy (1996) *Proc. Indian Acad. Sci. (Chem. Sci.)* **108**, 39–49.
21. D. C. Mitchell and B. J. Litman (1998) *Biophys, J.* **75**, 896–908.
22. C. R. Mateo, A. U. Acuna, and J. C. Brochon (1995) *Biophys. J.* **68**, 978–987.
23. C. Ho, M. B. Kelly, and C. D. Stubbs (1994) *Biochim. Biophys. Acta* **1193**, 307–315.
24. C. Ho, B. W. Williams, M. B. Kelly, and C. D. Stubbs (1994) *Biochim. Biophys. Acta* **1189**, 135–142.
25. G. Krishnamoorthy and A. Srivastava (1997) *Cell. Mol. Biol. Lett.* **2**, 145–163.
26. A. Srivastava and G. Krishnamoorthy (1997) *Curr. Sci.* **72**, 835–845.
27. Ira and G. Krishnamoorthy (1998) *Biochim. Biophys. Acta* **1414**, 255–259.
28. Ira and G. Krishnamoorthy (2001) *J. Phys. Chem. B.* **105**, 1484–1488.
29. C. R. Mateo, J. C. Brochon, M. P. Lillo, and A. U. Acuna (1993) *Biophys. J.* **65**, 2237–2247.
30. R. Varma and S. Mayor (1998) *Nature* **394**, 798–801.
31. T. Parasassi, G. Ravagnan, O. Sapora, and E. Gratton (1992) *Int. J. Radiat. Biol.* **61**, 791–796.
32. I. Konopasek, K. Strzalka, and J. Svobodova (2000) *Biochim. Biophys. Acta* **1464**, 18–26.
33. C. Bernsdorff, A. Wolf, R. Winter, and E. Gratton (1997) *Biophys. J.* **72**, 1264–1277.
34. A. M. Gilmore, V. P. Shinkarev, T. L. Hazlett, and G. Govindjee (1998) *Biochemistry* **37**, 13582–13593.
35. G. S. Laksmikanth, K. Sridevi, G. Krishnamoorthy, and J. B. Udgaonkar (2001) *Nature Struct. Biol.* **8**, 799–804.
36. L. M. S. Loura, A. Fedorov, and M. Prieto (2000) *J. Phys. Chem. B* **104**, 6920–6931.
37. M. D. Yeager and G. W. Feigenson (1990) *Biochemistry* **29**, 4380–4392.
38. D. R. James, J. R. Turnbull, B. D. Wagner, W. R. Ware, and N. O. Petersen (1987) *Biochemistry* **26**, 6272–6277.
39. D. B. Zimet, B. J. Thevenin, A. S. Verkman, S. B. Shohet, and J. R. Abney (1995) *Biophys. J.* **68**, 1592–1603.
40. T. R. Stouch and D. Bassolino (1996) *Biological Membranes: A Molecular Perspective from Computation and Experiment*, Birkhäuser, Boston, pp. 255–279.
41. E. Sackmann (1996) *Science* **271**, 43–48.
42. H. Evans and J. M. Graham (1989) in D. Richwood and D. Male (Eds.), *Membrane Structure and Functions*, IRL Press, Eynsham, UK, pp. 1–82.
43. J. F. Nagle and H. J. Morowitz (1978) *Proc. Natl. Acad. Sci. USA* **75**, 298.
44. H. S. Mei, M. E. Tuckerman, D. E. Sagnella, and M. L. Klein (1998) *J. Phys. Chem. B* **102**, 10446–10458.
45. C. Ho, S. J. Slater, and C. D. Stubbs (1995) *Biochemistry* **34**, 6188–6195.